A New Mechanistic Scenario for the Photochemical Transformation of Ergosterol: An MC-SCF and MM-VB Study

Fernando Bernardi,*,† Massimo Olivucci,‡ Ioannis N. Ragazos,‡ and Michael A. Robb*,‡

Contribution from the Dipartimento di Chimica "G. Ciamician" dell'Universita di Bologna, Via Selmi 2, 40126 Bologna, Italy, and Department of Chemistry, King's College, London, Strand, London WC2R 2LS, U.K. *Received November 18, 1991*

Abstract: The photochemical reaction network and photoequilibrium involved in the commercial synthesis of vitamin D and centered on ergosterol, precalciferol, lumisterol, tachysterol, and the toxisterols obtained by overirradiation have been studied using MM-VB. The six active electrons of the 1,3,5-hexatriene moiety are treated quantum mechanically via valence bond theory VB, and the remainder of the molecule is treated via molecular mechanics, MM. The results are then confirmed on the model system 1,3,5-hexatriene using MC-SCF computations at the 4-31G level with a CAS space of six orbitals and six electrons. A general mechanistic scenario that focuses on precalciferol as the *hub* of the photochemical reaction network and photoequilibrium has been documented. The central feature of this scenario is the existence of three "structural bottlenecks" through which the excited-state system must pass in order to return to the ground state. These structural bottlenecks are conical intersections or actual crossings of the ground and excited states where a fully efficient radiationless decay from the excited state to the ground state becomes possible. The optimized molecular structures at the conical intersections contain an integral allyl system located along the centers C_2–C_3–C_4 of the hexatriene moiety in two of the conical intersection structures and along the centers C_4–C_5–C_6 in the third. In both cases the carbon frame centered on the remaining carbon centers of the hexatriene moiety (i.e., C_1, C_4, and C_5 in one case and C_1, C_2, and C_3 in the other) is twisted or pyramidalized in such a way that the three sp hybrid orbitals are virtually orthogonal to each other and to the allylic system. These structures can be described as tetraradicaloid with three localized unpaired electrons and a fourth delocalized unpaired electron in an quasi-planar allyl-like fragment. The occurrence of the many different photorearrangement products in the precalciferol reaction network is completely rationalized by the many possible spin recouplings that can occur in this tetraradicaloid as it emerges on the ground-state surface at the conical intersection. Thus the main branches of the ergosterol photochemistry (leading to lumisterol and tachysterols) are based upon pathways involving the passage through these conical intersections.

Introduction

One of the textbook examples of the application of photochemistry in the fine chemical industry involves the synthesis of vitamin D using the photochemical electrocyclic ring opening of the 1,3-diene unit in ergosterol (E) to give precalciferol (P), which subsequently undergoes a thermal 1,7-H shift to produce vitamin D itself. However, the process is not clean because of the secondary absorption of P, which then undergoes further photochemical transformation via cis–trans isomerization to give rotamers of P itself or Z/E isomers and tachysterols (T) and via further electrocyclic reactions to give lumisterol (L), toxisterols, and E itself (Scheme I). This complex photochemical reaction network and photoequilibrium (and that of the model system 1,3,5-hexatriene) has been carefully documented as a result of several decades of experimental work,[1] and the most important results can be found in the comprehensive review of Havinga.[1a] General discussions of the photoequilibrium can be found in ref 2. The purpose of this paper is to document a new mechanistic scenario that complements and unifies the large amount of experimental data.

It is convenient to review the experimental results[1] using the triene precalciferol as the *hub* of the photochemical reaction and photoequilibrium network, from which cis–trans isomerism (rotation about C_2–C_3 and/or C_4–C_5 bonds), Z/E isomerization of the central (C_3–C_4) bond, and electrocyclic reactions are possible. (The cis–trans configuration of the central double bond (C_3–C_4) in conjugated trienes is specified using the symbols Z/E and that of the two lateral double bonds (C_2–C_3 and C_4–C_5) is specified using the symbols c/t. Thus the various rotamers are denoted cZc, cZt, etc.). For cis–trans isomerism about C_2–C_3 and C_4–C_5 bonds, experimental observations support the idea that the various conformers of a conjugated triene upon $\pi \rightarrow \pi^*$ excitation do not interconvert during their short (singlet) excited-state lifetime. This idea, which is known as *nonequilibration of excited rotamers* (NEER),[1a] has been used by photochemists for rationalizing distribution and quantum yields of triene photoproducts by correlating their structure to that of the most stable ground-state conformer of the reactant.[1b,e,2d] In other words, direct irradiation of a triene in its ground state would generate a distribution of excited-state conformers resembling the ground-state equilibrium distribution. This behavior has been explained on the hypothesis that an enhanced barrier for rotation in the excited state and a limited lifetime of the excited state make the overcoming of such a barrier unlikely. However, there is no mechanistic explanation for this process. Similarly, the actual mechanism of the other possible photorearrangements (Z/E isomerization of the central (C_3–C_4) bond and electrocyclic reactions) of conjugated trienes remains unclear. The direct irradiation of precalciferol leads to a quasi-photoequilibrium mixture of Z/E isomers (tachysterols) and cyclohexadienes (ergosterol and lumisterol) whose composition depends on the wavelength used in the experiment.[1c,d] Other cyclic compounds, corresponding to bicyclo[3.1.0]hex-2-enes (toxisterol C) and vinylcyclobutanes (toxisterol E), are formed via a more prolonged irradiation.[1a] From a mechanistic point of view, one

† "G. Ciamician" dell'Universita di Bologna.
‡ King's College, London.

(1) (a) Jacobs, H. J. C.; Havinga, E. Photochemistry of Vitamin D and Its Isomers and of Simple Trienes. Pitts, J. N., Jr., Hammond, G. S., Gollnick, K., Eds.; In *Advances in Photochemistry*; John Wiley & Sons: New York, 1979; Vol. 11, pp 305–373. (b) Dauben, W. G.; McInnis, E. L.; MIncho, D. M. Photochemical rearrangements in trienes. De Mayo, P., Ed. In *Rearrangements in ground and excited states*, Academic Press: London, 1980; Vol. 3, pp 91–129. (c) Malatesta, V.; Wills, C.; Hackett, P. A. *J. Am. Chem. Soc.* **1981**, *103*, 6781. (d) Dauben, W. G.; Phillips, R. B. *J. Am. Chem. Soc.* **1982**, *104*, 5781. (e) Brower, A. M.; Cornelisse, J.; Jacobs, H. J. C. *Tetrahedron* **1987**, *43*, 435. (f) Dauben, W. G.; Disanayaka, B.; Funhoff, D. J. H.; Kohler, B. E.; Schilke, D. E.; Zhou, B. J. *J. Am. Chem. Soc.* **1991**, *113*, 8367. (g) Petek, H.; Bell, A. J.; Christensen, R. L.; Yoshihara, K. *J. Chem. Phys.* **1992**, *96*, 2412.

(2) (a) Dauben, W. G.; Salem, L.; Turro, N. J. *Acc. Chem. Res.* **1975**, *8*, 41. (b) Grumbert, D.; Segal, G.; Devaquet, A. *J. Am. Chem. Soc.* **1975**, *97*, 6629. (c) Salem, L.; Leforestier, C.; Segal, G.; Wetmore, R. *J. Am. Chem. Soc.* **1975**, *97*, 479. (d) Turro, N. J. *Modern Molecular Photochemistry*; Benjamin Publishing: Reading, 1978. Gilbert, A.; Baggott, J. *Essentials of Molecular Photochemistry*; Blackwell Scientific Publications: Oxford, 1991. Coxson, J. M.; Halton, B. *Organic Photochemistry*; Cambridge University Press: London, 1974; pp 47–57. (e) Oosterhoff, L. J.; van der Lught, W. T. A. M. *J. Am. Chem. Soc.* **1969**, *91*, 6042.

0002-7863/92/1514-8211$03.00/0

Scheme I

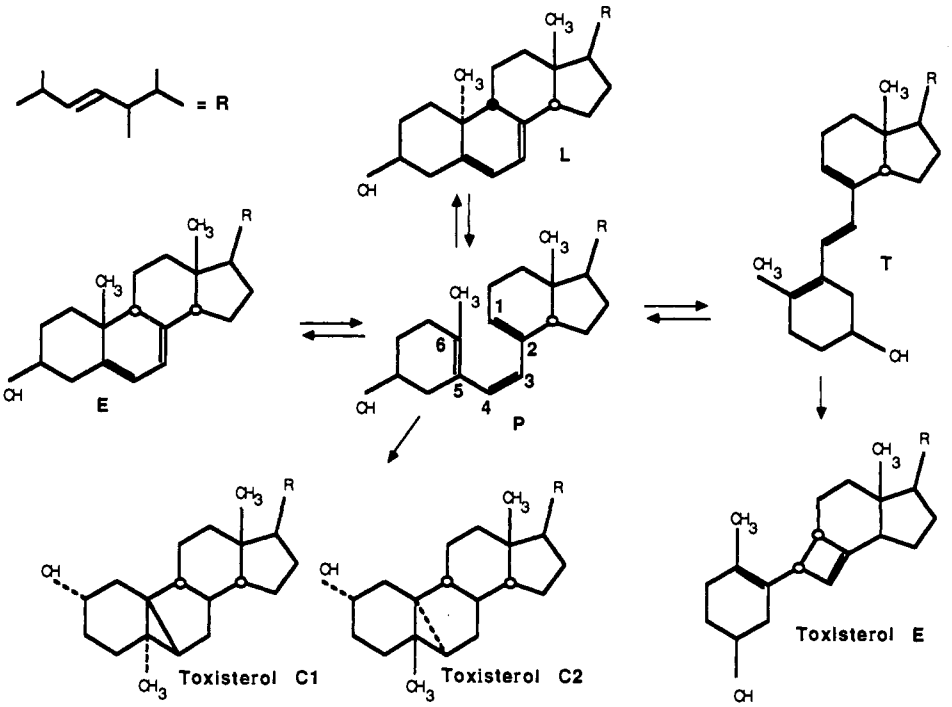

needs to understand how different photorearrangement products are generated by irradiating a single starting compound in its ground-state conformational equilibrium. The photorearrangement of parent hexa-1,3,5-trienes shows the same qualitative behavior of precalciferol.[1a,b] For instance, irradiation of hexa-1,3,5-triene, 2-methylhexa-1,3,5-triene, and 2,5-dimethylhexa-1,3,5-triene produces mixtures of Z/E isomers, cyclohexadienes, and the long-term irradiation products bicyclo[3.1.0]hexa-2-enes and vinylcyclobutanes plus products associated with hydrogen shifts. The quantum yield of these photoproducts depends on both the type of hexa-1,3,5-triene (i.e., type of substitution) and the wavelength used.[1e]

One must now state what one means by a mechanism for a photochemical reaction and how it can be documented with theoretical computations. We are concerned with nonadiabatic photochemical reactions that begin on an excited state and finish on the ground state. Thus it is clear that any photochemical mechanism for such reactions must have two stages, a stage that occurs on the excited state and a stage that occurs on the ground state. These two stages must be separated by a reaction *funnel* that occurs at the point where the excited state undergoes radiationless decay to the ground state. If this funnel is not accessible or does not exist (i.e., the gap between the ground and an excited state is so large that the probability of radionless decay is very small) then only an adiabatic reaction is possible. The position of this funnel determines the point at which the reaction emerges at a high-energy point on the ground-state surface and thus plays the central role in the determination of which products get formed. Thus in a photochemical mechanism we are concerned with reaction paths on the ground and excited state which can be characterized in the same way that one studies thermal reactions (i.e., location of intermediates and transition state geometries). The new problem in a photochemical mechanism is the characterization of the reaction funnel that must occur at the point where the excited state undergoes radiationless decay to the ground state.

The accepted model for the reaction funnel at the point where the excited state undergoes radiationless decay to the ground state involves an "avoided" crossing between ground and excited state.[1b,2] From a mechanistic point of view one is interested in the *position* of the funnel (i.e., the geometry of the system at the point where radiationless decay occurs) in the same way that one is interested in the structure of a transition state. The discussion in the standard textbooks is based upon the original treatment of Oosterhoff et al.[2e] where it assumed that the position of the effective funnel lies along the path of the ground-state-forbidden path. This qualitative model still forms the basis of the rationalization of modern experiments (see for example ref 1f). However, in recent work this model has been refined. We have shown[3c] that the reaction funnel can be a conical intersection[3] or an actual crossing of the ground and excited states. At a conical intersection, where ground- and excited-state surfaces actually cross, a fully efficient radiationless decay from the excited state to the ground state becomes possible (it has been demonstrated for realistic systems that the decay occurs rapidly within less than a vibrational period[3g]). The conical intersection is effectively a *structural bottleneck* because the system must assume the specific geometry of the conical intersection or the probability of radiationless decay is vanishingly small.

One of the central mechanistic problems in the photochemistry of trienes is how to rationalize the complex composition of the quasi-photoequilibrium mixture obtained by irradiating a single starting compound. On the one hand, one has the production of secondary products during the irradiation of the reactant arising from the secondary photoexcitation of the primary product. For instance, the intermediacy of (Z)-hexatrienes (precalciferol in Scheme I) in the production of (E)-hexatrienes (tachysterols) by irradiation of cyclohexa-1,3-dienes (ergosterol or lumisterol) has been unequivocally established. On the other hand, different primary products are simultaneously generated by irradiation of (Z)-hexatrienes or (E)-hexatrienes (precalciferol and tachysterols) even in conditions in which the investigators detect only one major equilibrium conformation for these two compounds. This second issue arises from the existence of efficient branching pathways in the decay of the photoexcited reactant to the ground state. As we will show later, the simultaneous production of various ground-state products can occur via two different mechanisms. The first mechanism is based upon the fact that structurally very different conical intersections are accessible from the flat excit-

(3) (a) Gerhartz, W.; Poshusta, R. D.; Michl, J. *J. Am. Chem. Soc.* **1977**, *99*, 4263. (b) Bonacic-Koutecky, V.; Koutecky, J.; Michl, J. *Angew. Chem., Int. Ed. Engl.* **1987**, *26*, 170–189. (c) Bernardi, F.; De, S.; Olivucci, M.; Robb, M. A. *J. Am. Chem. Soc.* **1990**, *112*, 1737–1744. (d) Davidson, R. E.; Borden, W. T.; Smith, J. *J. Am. Chem. Soc.* **1978**, *100*, 3299–3302. (e) Mead, C. A. The Born-Oppenheimer approximation in molecular quantum mechanics. Thruhlar, D. G., Ed. In *Mathematical frontiers in computational chemical physics*; Springer: New York, 1987; Chapter 1, pp 1–17. (f) Blais, N. C.; Thruhlar, D. G.; Mead, C. A. *J. Chem. Phys.* **1988**, *89*, 6204–6208. (g) Manthe, U.; Koppel, H. *J. Chem. Phys.* **1990**, *93*, 1658–1669.

Scheme II

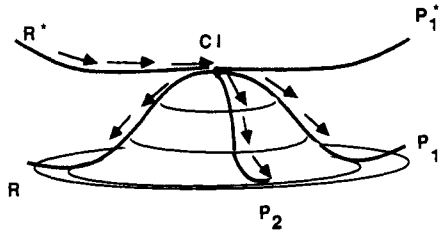

ed-state basin corresponding to the photoexcited reactant. Different ground-state products can then be formed via the decay from each of the structurally different *conical intersections*. The second mechanism arises because the reacting system emerges on the ground-state potential energy surface at what is loosely a *local maximum* where there is more than one downhill path. This situation is illustrated roughly in Scheme II. Because the excited system R* returns to the ground state via CI it can proceed downhill on the ground-state surface along one of several different paths, each one leading to several possible products R, P_2, P_1, etc. Dynamical considerations, the initial trajectory on the excited state, will clearly be very important in determining the actual ground-state path followed. The present theoretical computations can only demonstrate that such conical intersections exist and thus that certain pathways are possible.

Thus a reaction network for a photochemical reaction might involve several possible different competing excited paths leading to different structural bottlenecks (conical intersections) in the first stage of the reaction. Then the reaction paths can bifurcate on the ground-state part of the reaction pathway after the structural bottleneck and can lead to more than one product. A knowledge of geometric structures of the molecular system associated with a conical intersection should enable one to design photochemical reactions by blocking certain ground-state or excited-state paths by suitable substitution. For example, certain pathways that are accessible in hexa-1,3,5-triene photochemistry do not occur in precalciferol photochemistry.

Methodological Details

The location of excited- and ground-state critical point structures and structures corresponding to conical intersections for the precalciferol reaction network have been carried out using a new computational technique[4] (MM-VB), a combination of molecular mechanics methods (MM) and Heitler–London valence bond theory (VB). In this technique the six active electrons of the hexatriene fragment are treated using quantum mechanics (VB), and the remainder of the molecule is treated using MM. The topology of the precalciferol reaction network found using MM-VB was then confirmed via CAS-SCF/4-31G (six active electrons and six active orbitals) geometry optimizations on the parent hexa-1,3,5-triene. The ab initio calculations have been carried out using MC-SCF programs that are available in GAUSSIAN 91.[5] In agreement with experimental evidence we will assume that triplet excited states are not involved in the processes under investigation. Thus we will concentrate on the relationship between the ground state and the first covalent singlet excited state. In fact, it has now been established that the lowest excited state of *Z*-hexatrienes is the 2^1A_g covalent state.[6]

Now we briefly mention the practical aspects of the location of the lowest energy point on a conical intersection where the return to the ground state is possible. Two surfaces, even with the same symmetry, intersect in an $n-2$-dimensional hyperline. We are interested in the lowest energy point on this hyperline which corresponds to a well-defined geometry of the system. In order to properly locate the lowest energy point where two potential energy surfaces have the same energy, one must carry out a geometry optimization on the excited state with two constraints: (1) the energy of the two states must be equal and (2) the interaction matrix element between the two states must be zero. In this way we can search for a local minimum on a $n-2$-dimensional cross section of the n-dimensional potential energy surface (n = number of degrees of freedom of the system) which corresponds to the $n-2$-dimensional hyperline. We have recently developed such an optimization method and applied it to small model systems. The results are very similar to the simpler but approximate (and cheaper) procedure which has been applied in this study. This procedure uses the standard optimization methods for the search of a local minimum on the excited state. The optimization is stopped when the energy is stationary. The gradient will not be zero at such a point since a conical intersection point, on the excited-state potential energy surface, looks like the vertex of an inverted cone; however, the energy is minimized. This situation is distinguished from a "touching" of two surfaces where the gradient would go to zero. The approximate nature of the optimization method that we have used means that our conical intersection energies will be only upper bounds to the correct ones that one might obtain with a more accurate procedure.

Finally we must give some justification of the use of six active orbitals to describe the hexatriene system. The 175-term six-orbital MC-SCF wave function used for hexatriene is capable of describing all the states that can arise from all possible arrangements of six electrons in six orbitals. Our active space correlates with the 6 p^π orbitals of the planar hexatriene. *All the orbitals are fully utilized and optimized* in the computation, but only the active orbitals can have variable occupancy. Thus, no assumption of σ/π separability is implied. In the MM-VB method only the covalent states are explicitly described. However, the effect of ionic states is in fact included in this method as well via the parametrization against MC-SCF results. It is now accepted that the covalent 2^1A_g state is the lowest energy excited state in hexatrienes. Thus we would argue that we can describe the lowest energy excited state in both hexatriene and precalciferol itself. One could suggest that σ levels must intervene between the π levels in the ground-state planar arrangement and that all these must be included if σ/π mixing occurs. Indeed for some choice of an orbital Hamiltonian (say SCF) the occupied σ levels may indeed intervene between the π levels in the ground-state planar geometry; however, the σ orbitals will have double occupancy while the π orbitals will have variable occupancy (active space) in the various states. Thus the identification of 6 p^π active orbitals is merely a specification of which orbitals can have an occupancy other than 2 and does not imply anything at all about one-electron orbital energies. As the geometry is changed from a planar arrangement, the optimization of the orbitals mixes σ/π orbitals to give the lowest energy. The only type of interaction that is not included explicitly at the CI level would result from single excitations of the σ backbone. However, this type of interaction is included through the Brillouin condition satisfied by the optimum MC-SCF orbitals.

Results and Discussion

(i) General Mechanistic Scenario for the Precalciferol Reaction Network. We begin with a description of a general mechanistic scenario that focuses on precalciferol as the hub of the photochemical reaction network and photoequilibrium. The central feature of this scenario is the existence of three structural bottlenecks (i.e., conical intersections as discussed in the Introduction) through which the excited state must pass in order to return to the ground state. In subsequent subsections we shall document the various pathways in this scenario in more detail.

In Scheme III we give a general mechanistic scheme for the precalciferol reaction network that has as its key elements the three structural bottlenecks, the conical intersections, $CI_{c/t}{}^+$, $CI_{c/t}{}^-$, and $CI_{Z/E}$. The *solid* arrows indicate *ground*-state pathways while the *shaded* arrows indicate pathways on the *excited*-state surface. The structures corresponding to precalciferol (P) and related photoproducts (E, L, T, and toxisterol C1, C2, and E) represent schematic ground-state structures.

The MM-VB optimized structures corresponding to three minima on three different conical intersection regions reported in Scheme III are shown in Figure 1 ($CI_{c/t}{}^+$, and $CI_{c/t}{}^-$) and Figure 2 ($CI_{Z/E}$) while the CAS/4-31G and MM-VB geometries and CAS/4-31G energies of the parent hexatrienes are shown in Figure 3 parts a and b. The differences between the CAS/4-31G and MM-VB geometries give some indication of the accuracy of the MM-VB results. In particular, the torsional angles are very well produced by MM-VB. (Note that an excited-state transition structure for Z/E isomerism also exists with almost the same energy as shown in Figure 3c, and we shall return to discuss this later). These structures contain an almost integral system located along C_2–C_3–C_4 in the two structures $CI_{c/t}$ and along C_4–C_5–C_6

(4) Bernardi, F.; Olivucci, M.; Robb, M. A. *J. Am. Chem. Soc.* **1992**, *114*, 1606.

(5) Frisch, M. J.; Head-Gordon, M.; Trucks, G. W.; Foresman, J. B.; Schlegel, H. B.; Raghavachari, K.; Robb, M.; Wong, M. W.; Replogle, E. S.; Binkley, J. S.; Gonzalez, C.; Defrees, D. J.; Fox, D. J.; Baker, J.; Martin, R. L.; Stewart, J. J. P.; Pople, J. A. *Gaussian 91*, (*Revision C*); Gaussian, Inc.: Pittsburgh, PA, 1991.

(6) Bruma, W. J.; Kohler, B. E.; Song, K. *J. Chem. Phys.* **1991**, *94*, 6367.

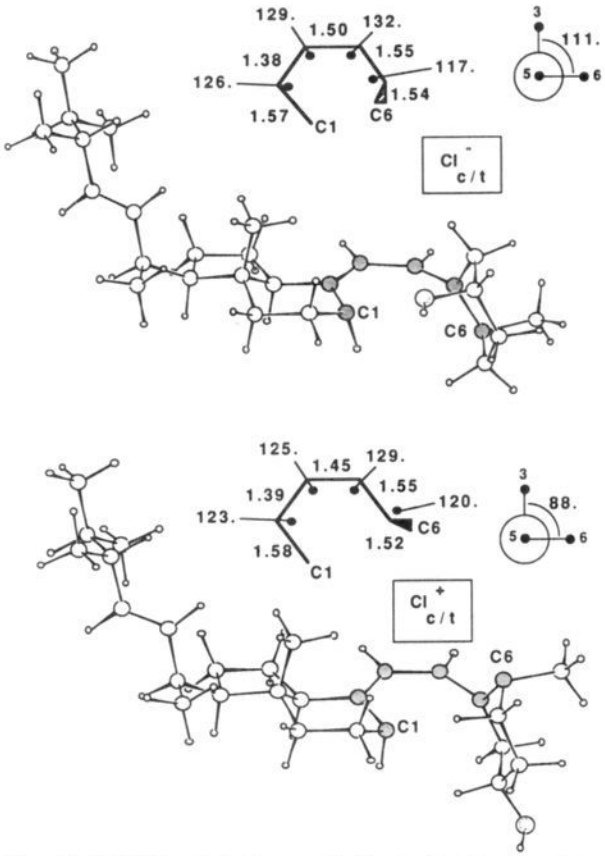

Figure 1. MM-VB optimized geometries for the $CI_{c/t}^{+/-}$ conical intersections in the precalciferol photochemical reaction network.

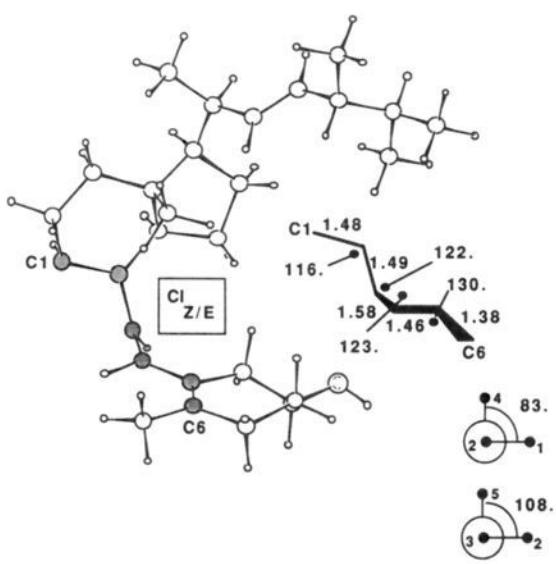

Figure 2. MM-VB optimized geometries for the $CI_{Z/E}$ conical intersection in the precalciferol photochemical reaction network.

in structure $CI_{Z/E}$. In both cases the carbon frame centered on the remaining carbon centers on the hexatriene moiety (i.e., C_1, C_5, and C_6 in $CI_{c/t}$ and C_1, C_2, and C_3 in $CI_{Z/E}$) is twisted or pyramidalized in such a way that the three sp hybrid orbitals are virtually orthogonal to each other and to the allylic system. These structures can be described as tetraradicaloid with three localized unpaired electrons and a fourth delocalized unpaired electron in a quasi-planar allyl-like fragment. We have used a simple VB model in ref 3c to rationalize the occurrence of such species.

Similarly, the MM-VB optimized ground-state structures of ergosterol and lumisterol (E and L in Scheme III) are shown in

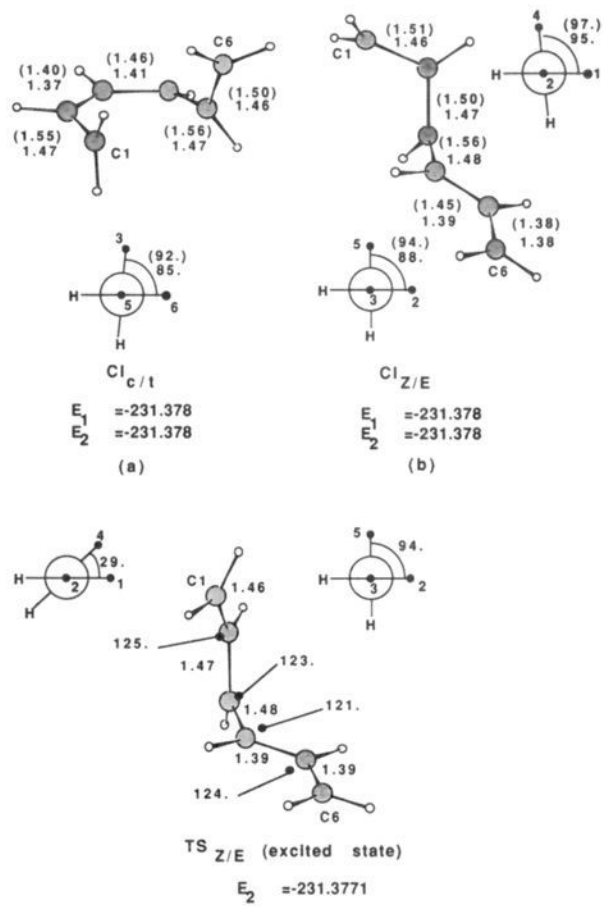

Figure 3. CAS-SCF/4-31G (six active electrons and six active orbitals) and MM-VB (in parentheses) optimized geometries for the $CI_{c/t}$ and $CI_{Z/E}$ conical intersections in the 1,3,5-hexatriene photochemical reaction network.

Figure 4. Precalciferol (P in Scheme III) can exist as two geometrical isomers c*Z*c and c*Z*t. The c*Z*c isomer has two diasteromers which we denote as c*Z*c$^+$ and c*Z*c$^-$. Their MM-VB optimized ground- and excited-state structures are shown in Figures 5, 6, and 7. The corresponding information for tachysterol (T in Scheme III) is given in Figure 8. The MC-SCF CAS/4-31G geometries and energies of the parent hexatrienes are shown in Figure 9.

The most important feature of this general mechanistic scheme is that, as already discussed in the Introduction, many ground-state paths are possible as the system emerges on the ground-state surface (see Scheme II) from the various conical intersections. For example, from $CI_{c/t}^+$ one can proceed to ergosterol, to two different isomers of precalciferol (c*Z*c$^+$ or c*Z*t), or to toxisterol. As a second example, two different photoproducts (precalciferol c*Z*c$^-$ and lumisterol) arise from the same conical intersection $CI_{c/t}^-$. The pathway actually followed will depend upon dynamical considerations determined partly by the initial trajectory on the excited-state surface. This remarkable situation results because the conical intersection is a tetraradicaloid. In fact, the four unpaired electrons of the tetraradicaloid structure at the conical intersection can recouple in different ways leading to bond formation. Thus a recoupling scheme can be associated with each ground-state relaxation pathway, which ultimately yields a specific photoproduct. This idea has been illustrated in Scheme IV where the recoupling processes which lead to ergosterol (E), precalciferol (P), and toxisterol starting from the $CI_{c/t}$ conical intersection have been labeled with the corresponding spin-coupling schemes. These same spin-coupling schemes have been used in Scheme III to indicate the recoupling process associated with the various ground-state relaxation pathways (solid arrows).

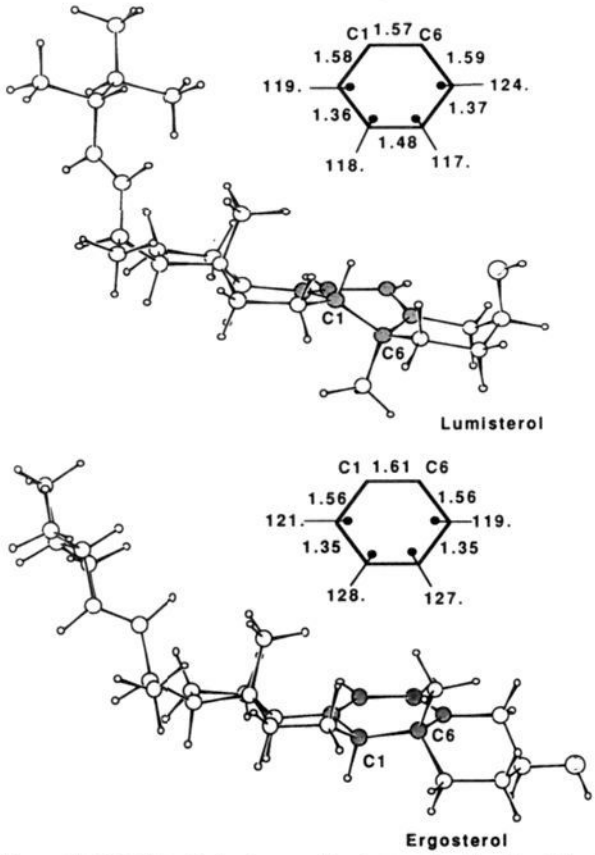

Figure 4. MM-VB optimized geometries for ergosterol and lumisterol.

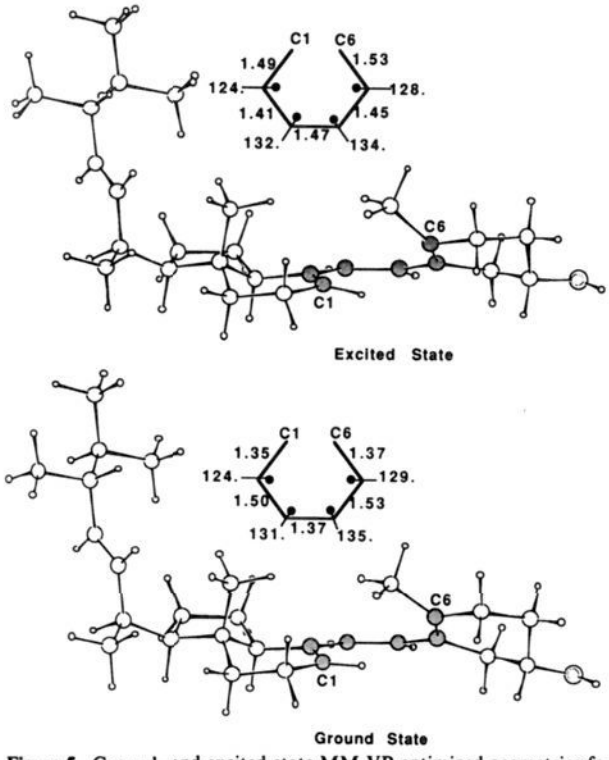

Figure 5. Ground- and excited-state MM-VB optimized geometries for cZc^+ precalciferol.

The existence of several possible pathways on the excited state provides the possibility of further mechanisms which are also compatible with simultaneous or competitive production of different photoproducts. Thus in general a different photoproduct can originate from several different excited-state pathways leading

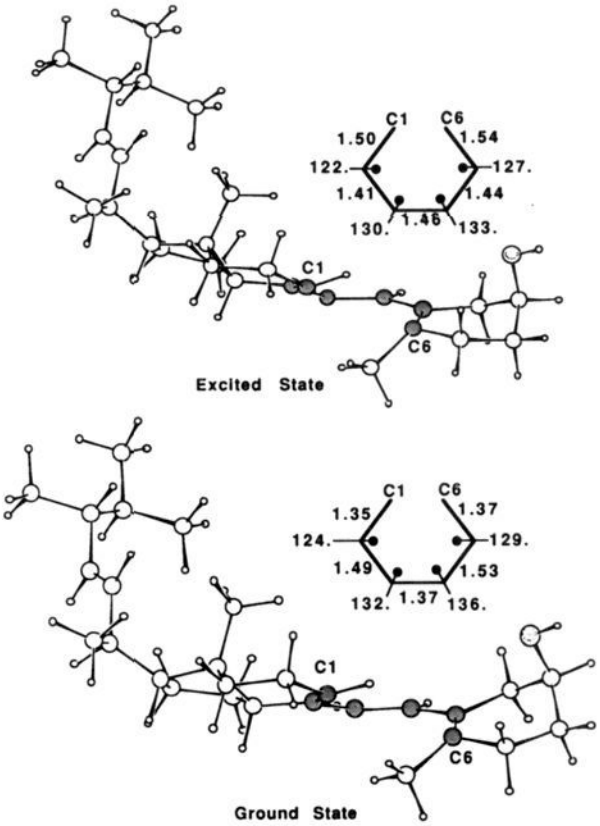

Figure 6. Ground- and excited-state MM-VB optimized geometries for cZc^- precalciferol.

to structurally different conical intersections or a single pathway whose passage through the conical intersection leads to a bifurcation of the reaction path on the ground-state sheet. We have just given an example of the second possibility in the scheme above. The first case is exemplified by the fact that the excited-state precalciferol conformer cZt* (the symbol cZt* indicates the excited-state conformer which is formed via absorption of a photon from the correspondent ground-state structure cZt) can evolve toward either the ground-state conformer cZc^- precalciferol (and related photoproducts) or the ground-state conformer c*E*t tachysterol through two structurally very different conical intersections ($CI_{c/t}^-$ and $CI_{Z/E}$). The initial stage of these processes is indicated by a dashed arrow in Scheme III. This arrow corresponds to the excited-state path starting from the excited-state conformer (generated via absorption of a photon) and leading to the conical intersection structure. In this situation the ratio between the global yields of cZc precalciferol and c*E*t tachysterol photoproducts will depend on the ratio between the barriers between the excited-state conformer and the conical intersections encountered following the two pathways.

Up to this point we have used precalciferol as the *hub* of the reaction network. The reaction paths proceeding toward precalciferol inward along one of the *spokes* need careful interpretation. The reaction of ergosterol to precalciferol via $CI_{c/t}^+$ is an example, and we shall discuss this in more detail later. Briefly, after photoexcitation of ergosterol the first stage of the reaction must take place on the excited state (dashed arrow in Scheme III) passing over any barriers to reach the decay point at $CI_{c/t}^+$. However, the vertical excitation of ergosterol places the system at a higher-energy point on the excited-state surface so these barriers are likely to be easily overcome and the reaction is quasi-concerned.

(ii) Cis–Trans (c/t) Isomerism in Precalciferol. Let us consider the MM-VB optimized structures of three excited-state and three ground-state precalciferol (c/t) rotamers shown in Figures 5, 6, and 7. The structure of the three excited-state minima differ from the corresponding ground-state structures in the values of the C–C

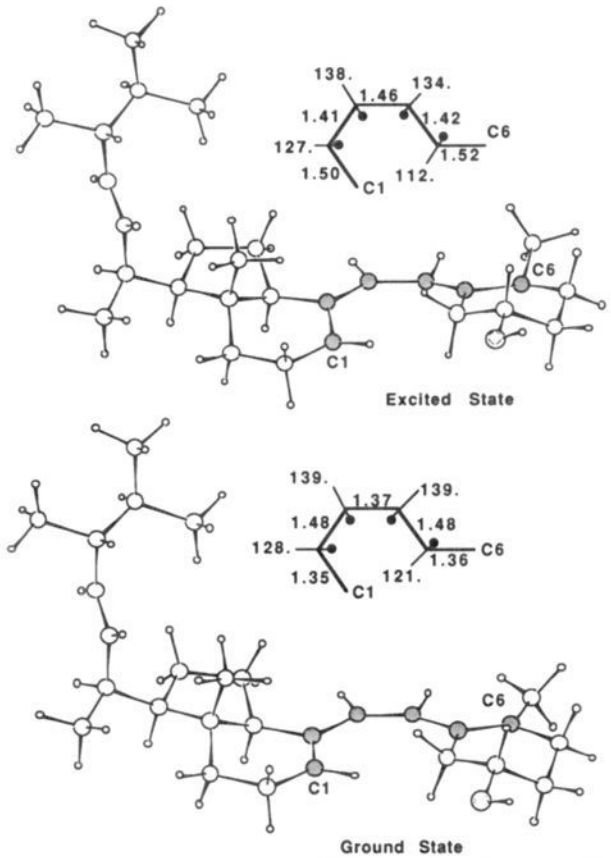

Figure 7. Ground- and excited-state MM-VB optimized geometries for c*Z*t precalciferol.

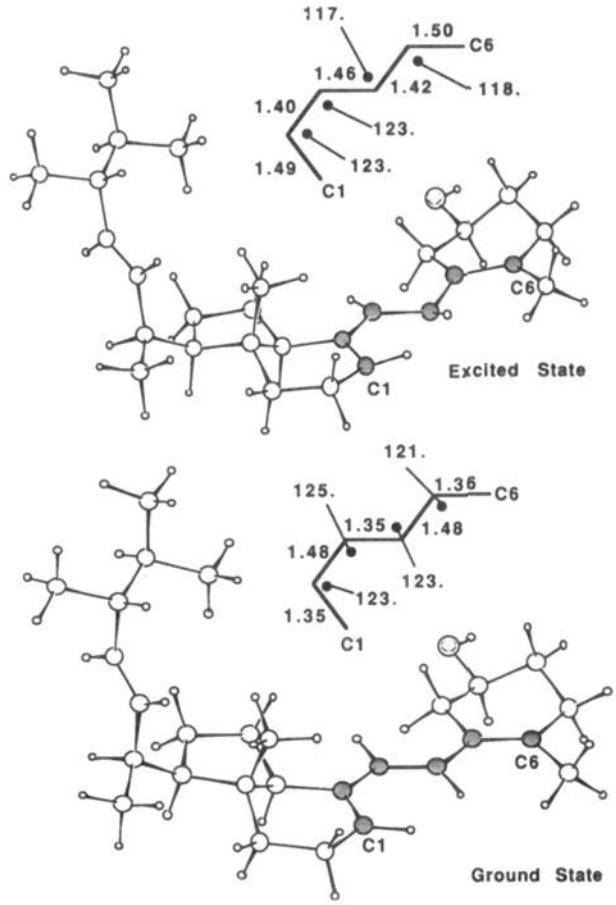

Figure 8. Ground- and excited-state MM-VB optimized geometries for c*E*t tachysterol.

bond lengths in the hexatriene moiety which are more uniform on the excited state. The same observation can be made for the geometries of the parent hexatrienes in Figure 9. Now we can observe that the conical intersection structures $CI_{c/t}$ are nearly coincident with "formal" transition structures for the interconversion of excited-state precalciferol rotamers. This is illustrated in Scheme V, which is intended to illustrate the surface topology in a qualitative fashion (only the excited- and ground-state stationary points and the CI have been located in the present study). Any search for the transition structures between the excited-state minima c*Z*c^{+*} or c*Z*c^{-*} and c*Z*t* leads toward two different regions in which the excited- and ground-state sheets are degenerate. In these "transition state" regions we find only the two conical intersection structures $CI_{c/t}^{+}$ and $CI_{c/t}^{-}$ (Figure 1). This observation is supported by the results of ab initio CAS-SCF/4-31G calculations on the parent system hexa-1,3,5-triene where the full π system (six electrons and six orbitals) has been included in the valence space. The two conical intersection structures $CI_{c/t}^{+}$ and $CI_{c/t}^{-}$ (see Figure 1) have structures virtually identical to the their corresponding MC-SCF hexatriene $CI_{c/t}$ counterpart (Figure 3a).

Thus the existence of the $CI_{c/t}$ conical intersection suggests a new way of explaining the short (singlet) lifetime of an excited-state conformer, as well as its inability to interconvert as stated by the NEER principle. The intercoverting conformer, for example, c*Z*c*, will have high probability to decay to the ground state through the conical intersection $CI_{c/t}$ before it could completely overcome the rotational barrier for interconverting to c*Z*t*. We have illustrated this feature qualitatively in Scheme VI. The coordinate that runs from bottom left to top left corresponds to c/t isomerization while the coordinate that runs from bottom left to bottom right corresponds to changes in C–C bond lengths. Thus the c*Z*t* and c*Z*t bond lengths are different and so the ground- and excited-state minima are displaced. The coordinate that runs from bottom left to bottom right corresponding to changes in C–C bond lengths is intended to represent these changes.

(iii) The *Z*/*E* Isomerism of Precalciferol and Tachysterol. The *Z*/*E* isomerism of precaciferol and tachysterol is similar to the cis–trans (c/t) isomerism of precalciferol except that a true c*Z*t* to c*E*t* transition state is found as well in the parent hexatriene (Figure 3c). The ground- and excited-state geometries of tachysterol c*E*t are shown in Figure 8 and those of the hexatriene structure in Figure 9c. Again the structure of the excited-state minima differs from the corresponding ground-state structure in the values of the C–C bond lengths in the hexatriene moiety, which are essentially equal on the excited state, and similarly for the geometry of the parent hexatriene. The geometry of the $CI_{Z/E}$ conical intersection can be found in Figure 2 with the corresponding ab initio result for hexatriene in Figure 3b. For hexatriene, we have also located a real transition structure (structure $TS_{Z/E}$ in Figure 3c) for the interconversion pathway from c*Z*t* precalciferol to c*E*t*, which does not lie on a touching region (ground–excited state energy separation greater than 50 kcal/mol). The eigenvector corresponding to the smallest *real* vibrational frequency of the system describes a rotation about C_5–C_6 which deforms the structure toward a ground–excited state touching region where the conical intersection structure $CI_{Z/E}$ (about 1 kcal/mol lower than the transition structure) has been located. Since the value of the frequency corresponding to this eigenvector is 113 cm^{-1}, the conical intersection region is readily accessible via a virtually free rotation about C_5–C_6.

(iv) Rationalization of Experimental Information. The fact that different touching regions between excited- and ground-state sheets are accessible via rotamer interconversion pathways on the excited-state sheet provides the foundation for a novel mechanistic scenario for the photochemistry of precalciferol and related compounds. According to this new scheme the various components of the mixture generated by direct irradiation of ergosterol are interconnected via different concerted excited state–ground state pathways passing through conical intersection structures which

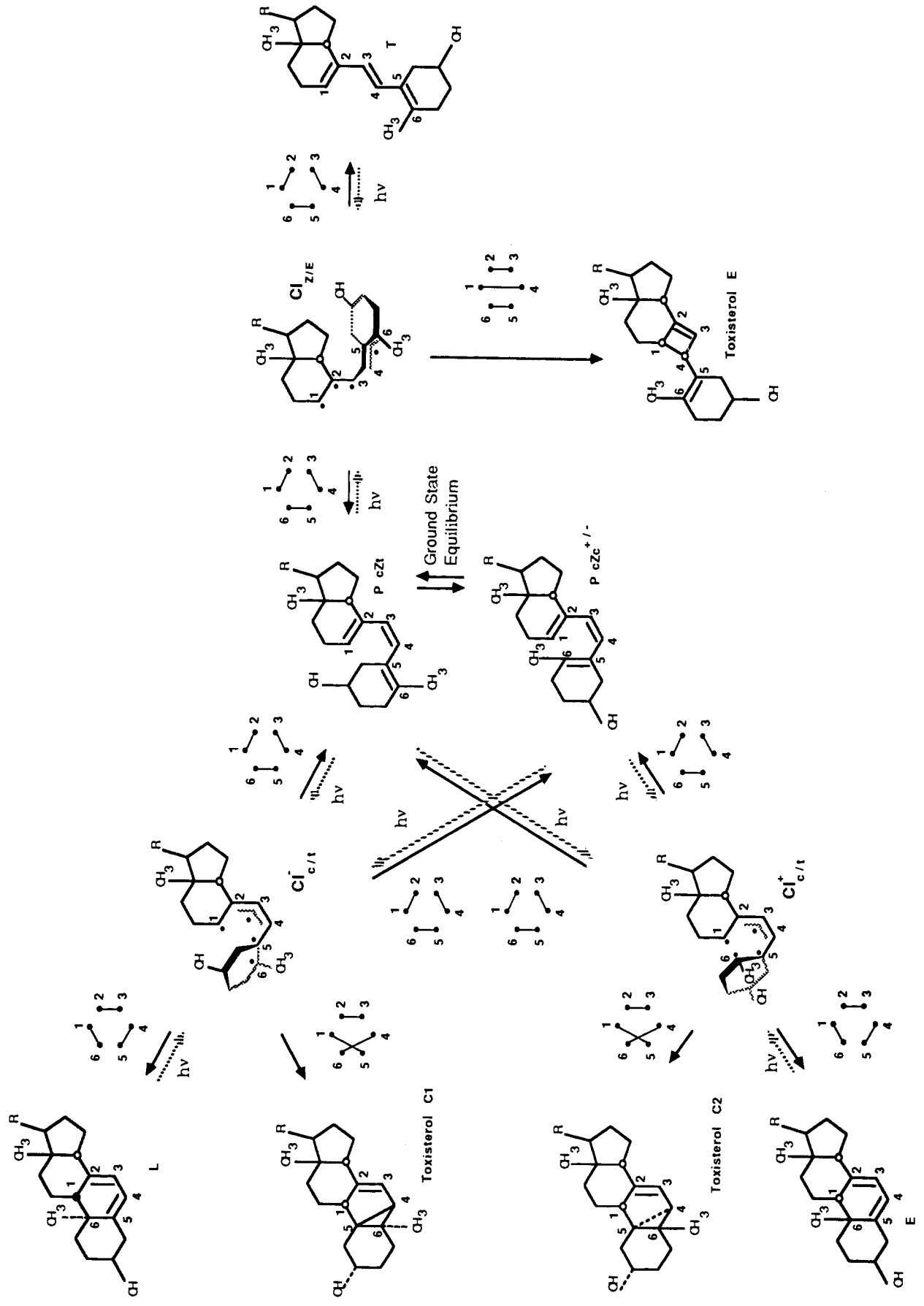
T
hν
Cl Z/E
Toxisterol E
Ground State Equilibrium
P cZt
P cZc+/-
Cl- c/t
Cl+ c/t
L
Toxisterol C1
Toxisterol C2
E

Scheme III

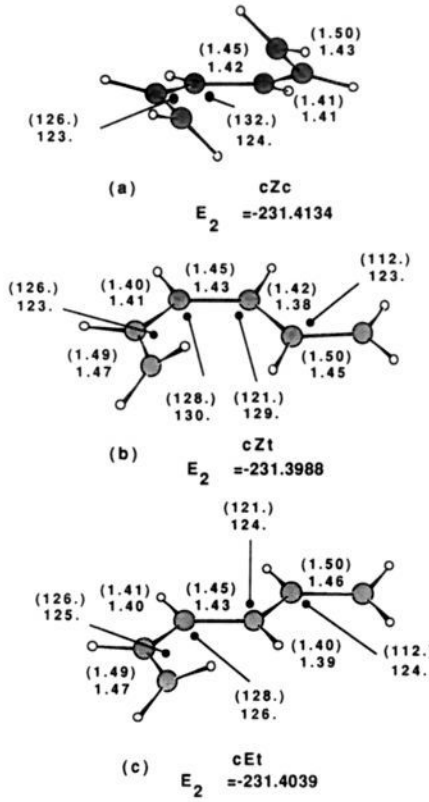

Figure 9. CAS-SCF/4-31G (six active electrons and six active orbitals) and MM-VB (in parentheses) optimized excited-state geometries for (a) cZc, (b) cZt, and (c) cEt isomers of the 1,3,5-hexatriene.

Scheme IV

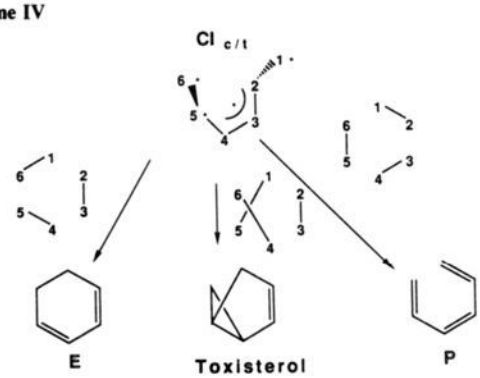

Scheme V

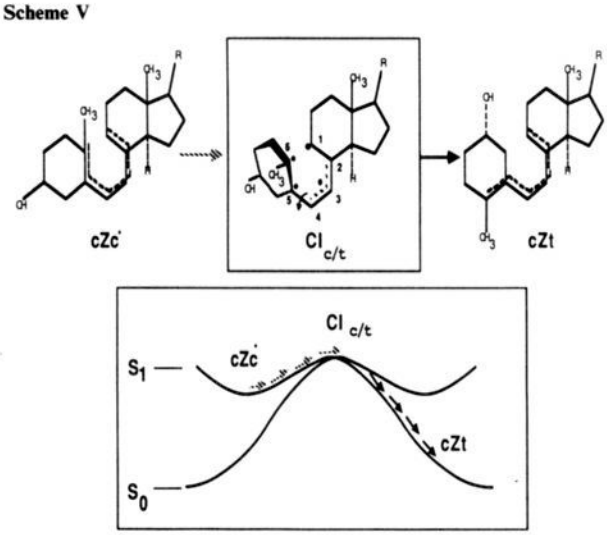

Scheme VI

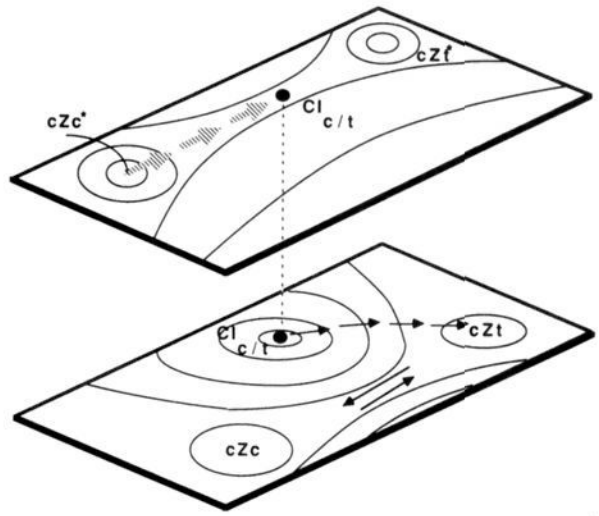

Scheme VII

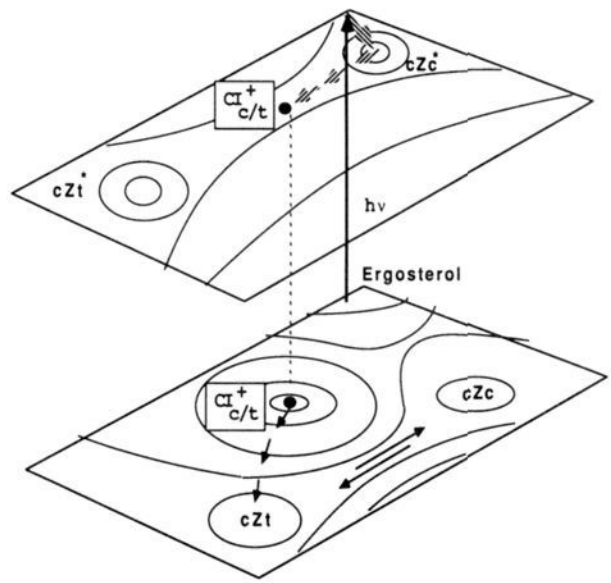

behave like structural bottlenecks. We will now discuss some of the pathways contributing to the complex photoequilibrium between ergosterol, precalciferol, luminsterol, and tachysterol. Our discussion will be based upon two main ideas. The first is that the irradiation of the reactants will populate the excited-state basin corresponding to the most stable ground-state conformers. Therefore, we can expect a highly populated cZt* basin if the cZt precalciferol dominates the conformational equilibrium mixture on the ground state. The second idea is that only certain structural bottlenecks are accessible from a specific excited-state basin so that only certain return pathways can be exploited for the return to the ground state.

The cZc^{+*} rotamer of precalciferol, which should be the primary product from direct irradiation of ergosterol, is formally interconnected to the rotamer cZt* via an excited-state pathway passing through the conical intersection $CI_{c/t}{}^{+}$ which is dominated by a 180° rotation about the C_4–C_5 bond. The situation is illustrated qualitatively in Scheme VII where an axis system similar to that of Scheme VI is used. The first stage of the reaction takes place on the excited state (dashed arrows). Upon photoexcitation, the ergosterol system arrives at a high-energy region of the excited-state surface and then evolves toward cZc^{+*}. Thus if the cZc^{+*} basin becomes populated via direct irradiation of ergosterol, the conical intersection will provide a very efficient route to ground-state precalciferol through the touching region. The only energetic barrier that the excited system must overcome is that

necessary to reach the conical intersection on the excited-state surface in the first stage of the reaction. For the parent system, this barrier (energy difference between cZc^{+*} and $CI_{c/t}$) has been evaluated using ab initio CAS-SCF/4-31G calculations on hexa-1,3,5-triene and has a value of 21 kcal/mol. After absorption of a 270-nm photon the system should have enough energy to be able to overcome this barrier easily. In fact, the excited-state energy evaluated at the ground-state optimized geometry of cyclohexadiene (which corresponds to a vertical Franck-Condon excitation) is 51 kcal/mol higher than the cZc^* minimum. The optimized geometries and energies of the hexa-1,3,5-triene rotamers corresponding to cZc^* ergosterol and to the conical intersection $CI_{c/t}$ are shown in Figure 9 and are essentially the same as those of the hexatriene moiety of the corresponding precalciferol rotamer. Note that the primary product of the photolysis of ergosterol can only be the production of precalciferol which will then tend to reach its conformational equilibrium in the ground state. Since the cZt^* rotamer is quasi-isolated from the cZc^* rotamer by the conical intersection point $CI_{c/t}$ which lies on their interconversion pathway, products from the decay of the cZt^* rotamer (e.g., via $CI_{Z/E}$) will not be generated except via secondary absorption of cZt itself.

The secondary absorption of the ground-state cZt rotamer of precalciferol should result in a production of cZt^* precalciferol which can undergo decay to the ground state according to different pathways. In fact the three different conical intersections shown in Scheme III are located along three different excited-state conformational interconversion pathways connecting the cZt^* to cZc^{+*}, cZc^{-*}, and cEt^* tachysterol. The decay through the first two conical intersections $CI_{c/t}^+$ and $CI_{c/t}^-$ results in the back production of ergosterol and in the production of lumisterol, respectively. These two transformations occur simultaneously with the production of cZc^+ and cZc^- precalciferol conformers since the decay pathway splits on the ground-state sheet acting to decrease the quantum yield for the ring-closure reactions. The third conical intersection ($CI_{Z/E}$) provides a decay pathway resulting in the formation of tachysterols which are the Z/E isomers of precalciferol. The presence of a rigid allyl system (C_4–C_5–C_6) in the structure of $CI_{Z/E}$ suggests that this decay pathway does not split toward precalciferols or ring-closure products supporting a relatively high quantum yield for the production of tachysterols. The excited-state energetics of these transformations has been investigated on the parent system hexa-1,3,5-triene via MC-SCF calculations, and the resulting optimized structures are shown in Figures 3 and 9. The difference in energy between the cZt^* rotamer and the $CI_{t/c}$ conical intersections is 13 kcal/mol while the difference between cZt^* and $CI_{Z/E}$ is 15 kcal/mol. Again the excited system should have enough energy to reach the conical intersections easily since the difference between the excited-state energy calculated at the optimized ground state cZt hexatriene geometry and the excited-state energy calculated at the optimized excited state cZt^* rotamer is 43 kcal/mol.

Two very recent experimental studies give some experimental confirmation of some very specific aspects of the conical intersection model that we have presented. Experimental work using fluorescence excitation spectra (Yoshihara et al.[1f]) on the parent *cis*-hexatriene demonstrates conclusively the existence of a fast nonradiative decay pathway that is associated with a low activation barrier which the authors assume involves Z/E isomerization. While we find that the energy of $CI_{Z/E}$ is 15 kcal/mol above cZt^*, within of the limitations of the optimization methods we use, the mechanism proposed in this work is consistent with these new results, while the older theory of Oosterhoff cannot begin to explain such observations. Yoshihara et al.[1f] also see a barrierless decay pathway. Our results suggest that this may be associated with the $CI_{c/t}$ conical intersection. The experiments of Dauben et al.[1f] on Ergosterol show an increased quantum yield for photocyclization at low photon energy (where the possible involvement of the 1B state is ruled out). Dauben et al. use the Oosterhoff model to rationalize their results in terms of a decay from an "avoided crossing" minimum. The results in the present work show that the reaction funnel is a conical intersection with a geometry very different from the one that they assume.

We now briefly discuss the production of the overirradiation products toxisterol C and toxisterol E. The mechanism for the production of these two steroids involves the two more strained decay pathways springing out (via a pathway bifurcation) from the conical intersections $CI_{c/t}$ and $CI_{Z/E}$, respectively. According to our mechanistic scheme (Scheme III), toxisterol C would be naturally formed via a decay pathway involving the spin recoupling of the three pairs of electrons on C_1 and C_5, C_2 and C_3, and C_4 and C_6. This type of pathway can be easily accessed from structures $CI_{c/t}$ (toxisterol C1 and C2 in Schemes I and III are generated from $CI_{c/t}^-$ and $CI_{c/t}^+$, respectively) via a five-membered ring closure involving the formation of a σ bond between C_1 and C_5 (the single occupied hybrid orbitals on C_1 and C_5 are facing each other). The production of toxisterol E1 requires the recoupling of the electron pairs C_1 and C_4, C_2 and C_3, and C_5 and C_6, which seems to be compatible with the structure of the conical intersection $CI_{Z/E}$. In fact this structure contains the butadiene moiety C_1–C_2–C_3–C_4 virtually identical to the proposed conical intersection for the electrocyclic ring closure of butadiene.[3c]

The composition of the photoequilibrium mixture of a hexatriene can be changed in two different ways (a) by changing the type of substitution on the hexatriene molecule (or type of constraints imposed by the carbocyclic skeleton in which the hexatriene moiety is embedded) or (b) by changing the radiation wavelength. While the complete quantitative rationalization of all the product composition data is beyond the capabilities of our model, the two effects find a natural basis for their rationalization in the mechanistic scenario discussed above. As we have already discussed, a different hexatriene structure can certainly make a decay pathway inaccessible by increasing the energy of certain conical intersections (which makes the knowledge of the conical intersection structures very important). On the other hand the change of substituents causes a different ground-state equilibrium distribution of hexatriene rotamers and in turn a different population of the excited-state rotamers which evolve toward different conical intersections. As a consequence the flux of the system on the excited-state sheet would be redistributed along different decay pathways (each one involving a conical intersection) causing a different final distribution of products. The wavelength dependence of the photoequilibrium composition can be rationalized in a similar way. In this case the relative population of the excited-state basins (each one corresponding to a different excited-state species) is not determined just by the equilibrium composition on the ground state but also by the different secondary absorption characteristics of the various ground-state compounds involved in the photoequilibrium. As an example, consider the Z/E photoisomerization at 353 nm. At this wavelength, tachysterol is the only compound having appreciable absorption. Irradiating tachysterol[1c] at 353 nm gives precalciferol as the only major photoequilibrium product while lumisterol and ergosterol are almost absent in the photoequilibrium mixture. This result is explained by a mechanism involving the production of excited-state tachysterol that then decays through the conical intersection $CI_{Z/E}$ producing precalciferol and the long term irradiation toxisterol E. The weak secondary absorption of precalciferol and consequent low population of the precalciferol excited-state basin explain the almost complete absence of lumisterol and ergosterol in the photoequilibrium mixture which would be produced via decay through $CI_{c/t}$.

Conclusions

A general mechanistic scenario that focuses on precalciferol as the hub of the photochemical reaction network and photoequilibrium of ergosterol, precalciferol, lumisterol, tacysterol, and the toxisterols has been documented. The central feature of this scenario is the existence of three structural bottlenecks through which the excited state must pass in order to return to the ground state. These structural bottlenecks are conical intersections or actual touchings of the ground and excited states where a fully efficient radiationless decay from the excited state to the ground state becomes possible. The molecular structures associated with

the structural bottlenecks can be described as tetraradicaloid with three localized unpaired electrons and a fourth delocalized unpaired electron in an quasi-planar allyl-like fragment. The occurrence of the many different photorearrangement products in the precalciferol reaction network is completely rationalized by the many possible spin recouplings that can occur in this tetraradicaloid as it emerges on the ground-state surface at the conical intersection. Thus the main branches of the ergosterol photochemistry (leading to lumisterol and tachysterols) can be rationalized via pathways involving the passage through these conical intersections.

Acknowledgment. This work was supported by the SERC (UK) under grant numbers GR/F 48029, 46452, and GR/G 03335. All ab initio computations were carried using MC-SCF programs that are available in GAUSSIAN 91.[5]

The Conformations of Proline-Linked Donor-Acceptor Systems

Scott F. Sneddon*,† and Charles L. Brooks III‡

Contribution from Pfizer Central Research, Groton, Connecticut 06340, and the Department of Chemistry, Carnegie Mellon University, Pittsburgh, Pennsylvania 15213.
Received December 27, 1991

Abstract: We have carried out a simulation study of the stable conformations of Pro–Pro peptides in solution, and of Pro_n peptides (where n = 1–4) in a dielectric continuum model, to explain the observed electron-transfer rates in proline-linked donor–acceptor systems studied by Isied and Vassilian.[1] They found that the rate of electron transfer in proline-linked donor–acceptor systems decreases by the expected amount for Pro_2 versus Pro_1, but for Pro_3 and Pro_4 the rate increases, with Pro_4 having the fastest transfer rate of the peptides studied. This finding suggests that conformational flexibility in the longer peptides enables the donor and acceptor to reach short transfer distances, resulting in the faster transfer rate. We have performed conformational free energy simulations to determine the free energy barriers for transitions of the backbone degrees of freedom of Pro–Pro peptides in solution. From the stable structures found we have carried out simulations of the Pro_1-to-Pro_4-linked donor–acceptor systems to determine the structural changes that best explain the observed trend in the electron-transfer rates. We found that the proline secondary structures poly(Pro)I and poly(Pro)II cannot explain the trend in transfer rates and that, instead, transitions of the ψ backbone dihedral from an extended to an α conformation can give short enough transfer distances to explain the experimental rates. Our analysis suggests that transitions of the backbone ψ dihedral angle represent a significant mechanism for conformational change in proline peptides.

In this paper we discuss the influence of conformational flexibility on the rate and pathway of electron transfer in proline-linked donor–acceptor systems. Experimental studies have shown that the rate of transfer is not a simple function of the length of the peptide joining the donor and acceptor.[1,2] Rather, the rate first decreases with chain length and then begins to increase as the chain is lengthened (Table I). Since the covalent through-bond path increases with chain length, there can be two arguments to explain this observation. Either the longer chain can fold back on itself to bring the donor and acceptor closer or through-bond coupling becomes more efficient as the chain is lengthened.[3] In their first studies of this system Isied and Vassilian discussed the former cause and suggested that a conformational change to the poly(Pro)I structure[4,5] might explain the faster rates of the Pro_3 and Pro_4 peptides. More recently, they have discussed the latter cause, attributing the change in rate to more efficient electronic coupling for the amide group in the longer peptides (specifically in the all cis conformation of the backbone).[3] Our calculations of the tunneling barrier height of amides do not support a significant change in the electronic coupling for the two conformations, so we have explored the role of conformational change in enhancing the rate in the longer peptides.

Proline is a unique amino acid in two important ways. First, the covalent link between C^α and the amino nitrogen greatly reduces the rotational freedom of the backbone ϕ angle. Second, the lack of an amide proton makes the cis and trans conformations of the ω dihedral closer in free energy than in all other amino acids.[6,7] The dihedral angles ϕ, ψ, and ω, are shown in proline. Proline peptides adopt two types of regular backbone structure characterized by the value of ω. The right-handed helical form, poly(Pro)I, has all cis peptide bonds, while for the left-handed

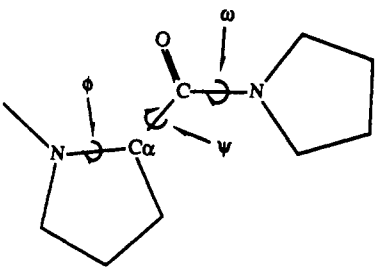

helical form of poly(Pro)II the peptide bonds are trans. In both of these conformations the ψ dihedral is in the extended, or β, conformation.[4] At pH 7 the all-trans poly(Pro)II is the more stable species.[6,7]

To determine how proline peptides can change conformation we computed gas-phase potential energy surfaces for both backbone degrees of freedom in proline: ψ and ω. We found that each dihedral has two stable minima: the cis and trans conformation of the ω dihedral and the α and β conformations of the ψ dihedral. We used potential of mean force (pmf) calculations to characterize the free energy for transitions between these stable structures in aqueous solvent. We found that gas-phase calculations that em-

† Pfizer Central Research.
‡ Carnegie Mellon University.

(1) Isied, S. S.; Vassilian, A. *J. Am. Chem. Soc.* **1984**, *106*, 1732–1736.
(2) Isied, S. S.; Vassilian, A. *J. Am. Chem. Soc.* **1984**, *106*, 1726–1732.
(3) Isied, S. S. In *200th ACS National Meeting*; Washington D.C., 1990; p 103.
(4) Richardson, J. S. *Adv. Protein Chem.* **1981**, *34*, 167–339.
(5) Creighton, T. E. *Proteins, Structures and Molecular Properties*; W. H. Freeman and Co.: New York, 1983.
(6) Thomas, W. A.; Williams, M. K. *J. Chem. Soc., Chem. Commun.* **1972**, 994.
(7) Evans, C. A.; Rabenstein, D. L. *J. Am. Chem. Soc.* **1974**, *96*, 7312–7317.

0002-7863/92/1514-8220$03.00/0